

9-8-2021

Sympathoinhibition and vasodilation contribute to the acute hypotensive response of the superoxide dismutase mimic, MnTnBuOE-2-PyP5+, in hypertensive animals

Sarah L. Schlichte

Elizabeth J. Pekas

Taylor J. Bruett

Elizabeth A. Kosmacek

Bryan T. Hackfort

See next page for additional authors

Follow this and additional works at: <https://digitalcommons.unomaha.edu/hperfacpub>



Part of the [Health and Physical Education Commons](#), and the [Kinesiology Commons](#)

Please take our feedback survey at: https://unomaha.az1.qualtrics.com/jfe/form/SV_8cchtFmpDyGfBLE

Authors

Sarah L. Schlichte, Elizabeth J. Pekas, Taylor J. Bruett, Elizabeth A. Kosmacek, Bryan T. Hackfort, Jordan M. Rasmussen, Kaushik P. Patel, Song-young Park, Rebecca E. Oberley-Deegan, and Matthew C. Zimmerman



Full Length Article

Sympathoinhibition and vasodilation contribute to the acute hypotensive response of the superoxide dismutase mimic, MnTnBuOE-2-PyP⁵⁺, in hypertensive animals



Sarah L. Schlichte^a, Elizabeth J. Pekas^b, Taylor J. Bruett^a, Elizabeth A. Kosmacek^c, Bryan T. Hackfort^a, Jordan M. Rasmussen^a, Kaushik P. Patel^a, Song-Young Park^b, Rebecca E. Oberley-Deegan^c, Matthew C. Zimmerman^{a,*}

^a Department of Cellular and Integrative Physiology, University of Nebraska Medical Center, Omaha, NE

^b School of Health and Kinesiology, University of Nebraska Omaha, Omaha, NE

^c Department of Biochemistry and Molecular Biology, University of Nebraska Medical Center, Omaha, NE

ARTICLE INFO

Keywords:

MnTnBuOE-2-PyP⁵⁺
Hypertension
Superoxide Dismutase
Sympathetic Nerve Activity
Vasodilation

ABSTRACT

The pathogenesis of hypertension has been linked to excessive levels of reactive oxygen species (ROS), particularly superoxide ($O_2^{\bullet-}$), in multiple tissues and organ systems. Overexpression of superoxide dismutase (SOD) to scavenge $O_2^{\bullet-}$ has been shown to decrease blood pressure in hypertensive animals. We have previously shown that MnTnBuOE-2-PyP⁵⁺ (BuOE), a manganese porphyrin SOD mimic currently in clinical trials as a normal tissue protector for cancer patients undergoing radiation therapy, can scavenge $O_2^{\bullet-}$ and acutely decrease normotensive blood pressures. Herein, we hypothesized that BuOE decreases hypertensive blood pressures. Using angiotensin II (AngII)-hypertensive mice, we demonstrate that BuOE administered both intraperitoneally and intravenously (IV) acutely decreases elevated blood pressure. Further investigation using renal sympathetic nerve recordings in spontaneously hypertensive rats (SHRs) reveals that immediately following IV injection of BuOE, blood pressure and renal sympathetic nerve activity (RSNA) decrease. BuOE also induces dose-dependent vasodilation of femoral arteries from AngII-hypertensive mice, a response that is mediated, at least in part, by nitric oxide, as demonstrated by *ex vivo* video myography. We confirmed this vasodilation *in vivo* using doppler imaging of the superior mesenteric artery in AngII-hypertensive mice. Together, these data demonstrate that BuOE acutely decreases RSNA and induces vasodilation, which likely contribute to its ability to rapidly decrease hypertensive blood pressure.

Introduction

Hypertension affects approximately 45% of American adults and only about 25% of affected individuals have their blood pressure under control [1]. Additionally, hypertension is a leading risk factor for a variety of cardiovascular-related diseases including myocardial infarction, stroke, heart failure, and kidney disease [1, 2]. Thus, novel anti-hypertensive therapeutics are needed to help patients with uncontrolled hypertension lower their blood pressure and minimize their risk of developing other cardiovascular morbidities.

Over the past two decades, the connection between hypertension and reactive oxygen species (ROS), particularly superoxide ($O_2^{\bullet-}$) has become well established [3–5]. Angiotensin II (AngII), the primary effector peptide of the renin-angiotensin system, increases $O_2^{\bullet-}$ levels in

multiple organs, including the brain, kidney, and the vasculature. The resulting sympathoexcitation [6, 7], renal dysfunction [8], and vasoconstriction [9] are known to contribute to the pathogenesis of hypertension [10]. Endogenously, $O_2^{\bullet-}$ is specifically scavenged by a family of three enzymes known as superoxide

Dismutase (SOD). Previous work in our laboratory and others has shown that scavenging $O_2^{\bullet-}$ *in vivo* via overexpression of SOD or administration of SOD mimics decreases blood pressure in hypertensive animals [11–14]. Unfortunately, the transition of these potentially therapeutic anti-hypertensive strategies to the clinical setting has been delayed for various reasons.

One particular SOD mimic that has advanced into multiple clinical trials is MnTnBuOE-2-PyP⁵⁺ (BuOE). This redox-active manganese porphyrin is being clinically evaluated (ClinicalTrials.gov Identifiers:

* Corresponding author at: Integrative Physiology & Molecular Medicine Doctoral Program, Director, Free Radicals in Medicine Program, Department of Cellular and Integrative Physiology, University of Nebraska Medical Center, 985850 Nebraska Medical Center, Omaha, NE 68198-5850. Phone: 402-559-7842 (office).

E-mail address: mczimmerman@unmc.edu (M.C. Zimmerman).

<https://doi.org/10.1016/j.arres.2021.100016>

Received 24 June 2021; Received in revised form 18 August 2021; Accepted 23 August 2021

Available online 27 August 2021

2667-1379/© 2021 The Author(s). Published by Elsevier B.V. This is an open access article under the CC BY-NC-ND license (<http://creativecommons.org/licenses/by-nc-nd/4.0/>)

NCT02655601, NCT02990468, NCT03386500, NCT03608020) for its ability to act as a radioprotector of normal tissue while suppressing tumor growth in cancer patients receiving radiation therapy [15]. The enhanced lipophilicity and reduced toxicity of BuOE relative to other manganese porphyrins such as MnTE-2-PyP (T2E) has contributed to its clinical advancement and also prompted the study of BuOE in other disease models [16–18]. Recent work from our lab showed that BuOE decreases normotensive blood pressures in mice [19]. This work is in agreement with non-clinical safety and toxicity studies showing that BuOE significantly decreases blood pressure in dogs [20]. Furthermore, BuOE has also been investigated in aortic valve stenosis [21], a clinical manifestation that is associated with hypertension. However, the effect of BuOE on hypertensive blood pressures remains unknown.

Considering the extensive knowledge of the role of $O_2^{\bullet-}$ in hypertension [3, 10], previous work demonstrating BuOE's ability to scavenge $O_2^{\bullet-}$ [16, 18, 19] and decrease normotensive blood pressures [19], we tested the hypothesis that BuOE decreases hypertensive blood pressures in AngII-hypertensive mice, as well as spontaneously hypertensive rats (SHRs), and further sought to examine the mechanism(s) behind the BuOE-induced hypotensive response. Herein, we report that BuOE induces an immediate and transient decrease in blood pressure in AngII-hypertensive mice and SHRs mediated, at least in part, by sympathoinhibition and vasodilation.

Materials and methods

Animals

Ten-week-old male C57Bl/6 mice (23–27 g, Jackson Laboratories, Bar Harbor, ME) were housed in the animal facility at the University of Nebraska Medical Center (UNMC) with access to standard chow and water ad libitum on a 12-h light-dark cycle. Blood pressure, myography, and doppler imaging experiments were conducted following a one-week acclimatization period at the UNMC animal facility.

Eighteen-week-old male Wistar Kyoto (WKY) rats and aged-matched Spontaneously Hypertensive Rats (SHRs) (315–360 g, Charles River Laboratories, Wilmington, MA) were used to record normotensive (control) and hypertensive renal sympathetic nerve recordings, respectively. Rats were group-housed in the animal facility with access to standard chow and water ad libitum on a 12-h light-dark cycle. Upon arrival, rats were allowed to age to eighteen weeks old and acclimate to the UNMC facility.

All procedures were performed in accordance with institutional guidelines for animal research reviewed and approved by the University of Nebraska Medical Center Institutional Animal Care and Use Committee.

BuOE preparation

BuOE (a generous gift from Dr. James Crapo from National Jewish Health, Denver, CO) powder was kept under a vacuum seal at room temperature away from moisture and light. The drug was weighed out, reconstituted with PBS, and sterilized with a 0.2 μ M PES syringe filter (Basix, Thermo Fisher Scientific, Hampton, NH). The molarity of the solution was determined by spectrophotometer prior to sterilization.

Blood pressure measurements

Mice were implanted with radiotelemeters (PhysioTel PA-C10, Data Sciences International, St. Paul, MN), as previously described [13, 19, 22], to record blood pressure. Briefly, mice were anesthetized with isoflurane inhalation (2.5%) and kept under anesthesia by isoflurane inhalation (1–2%) for the duration of the procedure. Once the left carotid artery was isolated, the catheter of the telemeter was inserted into the carotid artery and secured with 7–0 braided silk sutures (Teleflex Medical, Coventry, CT). The body of the telemeter was placed in a subcu-

aneous pouch on the right side of the mouse. The incision was closed with 6.0 Prolene suture (Ethicon, Cincinnati, OH) and treated with bupivacaine (1 mg/kg, subcutaneous) immediately following the procedure. Mean arterial pressure (MAP), systolic blood pressure (SBP), and diastolic blood pressure (DBP) were recorded daily in single-housed, conscious, unrestrained mice.

Once a consistent normotensive baseline blood pressure was achieved for three consecutive days, mice were implanted subcutaneously with osmotic minipumps (Alzet #1002, Durect Corporation, Cupertino, CA) delivering AngII (Sigma #A9525, St. Louis, MO) to induce hypertension [13, 22, 23]. Pumps infused 400 ng/kg/min AngII for approximately 3 weeks until the pumps emptied.

When mice became hypertensive (around Day 10 of AngII infusion), they were intraperitoneally (IP) or intravenously (IV) injected with 100 μ L of vehicle (saline) or BuOE (IP: 1.0, 5.0 mg/kg; IV: 0.1, 0.5, 1.0 mg/kg). Upon completion of the studies, mice were euthanized with an overdose of pentobarbital (150 mg/kg, IP).

Renal nerve recordings

Renal sympathetic nerve recordings were performed as previously described [19, 24, 25]. On the day of the recording, rats were anesthetized with an IP injection of urethane (0.75 g/kg) and α -chloralose (70 mg/kg). The right femoral artery was cannulated with PE-50 polyethylene tubing connected to a pressure transducer (PowerLab Data-Acquisition System, ADInstruments, Colorado Springs, CO) to measure MAP and heart rate (HR), while the right femoral vein was cannulated to administer the drugs IV. A tracheal intubation was performed to allow for independent breathing. The left kidney was exposed via a retroperitoneal flank incision and the renal artery and vein were identified. After a branch of the renal nerve was isolated and placed on a bipolar electrode, the nerve/electrode junction was surrounded with WACKER SilGel mixture (604 & 601). This isolation of the junction reduced the noise to signal ratio and prolonged the duration of a good signal. The electrical signal was amplified via a Grass amplifier with high- and low-frequency cutoffs of 1000 Hz and 100 Hz, respectively. The rectified output (resistor capacitor) filtered time constant (0.5 s) was then recorded and integrated using PowerLab (8si, ADInstruments, Sydney, NSW, Australia). Following approximately 30 min of stable baseline recording, BuOE (0.5 mg/kg, IV) was administered and changes in MAP, HR, and RSNA were monitored. Following the completion of this protocol, hexamethonium (120 mg/mL, IV) was administered to determine the amount of background noise in the signal. Basal nerve activity was determined at the beginning of the experiment, and background noise was determined by nerve activity recorded at the end of the experiment. To calculate the RSNA during the experiment, the background noise was subtracted from the recorded value. The RSNA response to drugs was expressed as a percentage change from the basal value.

Electron paramagnetic resonance (EPR) spectroscopy

EPR spectroscopy and the cell permeable superoxide-sensitive spin probe, 1-hydroxy-3-methoxycarbonyl-2,2,5,5-tetramethylpyrrolidine (CMH), were used to measure $O_2^{\bullet-}$ levels in femoral arteries collected from normotensive or AngII hypertensive mice. Immediately upon harvesting the femoral artery from the mouse hind limb, the tissue was placed in warm (37 °C) Krebs-HEPES buffer containing deferoxamine methanesulfonate salt (DF, 25 μ M) and diethyldithiocarbamic acid sodium salt (DETC, 5 μ M). CMH (200 μ M) was added, and samples were incubated at 37 °C for 1 h. Then, samples were frozen in liquid nitrogen, placed into a liquid nitrogen finger dewar, and inserted into the resonator cavity of a Bruker eScan EPR spectrometer. Directly proportional to the level of free radicals (i.e., $O_2^{\bullet-}$) in the sample, the EPR spectra amplitude in arbitrary units was normalized to tissue weight.

Video myography

Video myography was performed as previously described [26, 27]. Briefly, the femoral artery at the femoral to popliteal artery junction was isolated from the hind limb of normotensive and AngII-hypertensive mice. Adipose and connective tissues surrounding the arteries were removed under a microscope (SZX10; Olympus, Center Valley, PA) in 4 °C physiological saline solution (PSS) [containing (in mM) 138.0 NaCl, 4.0 KCl, 1.2 MgSO₄ anhydrous, 1.6 CaCl₂×2H₂O, 1.2 KH₂PO₄, 0.026 EDTA, 6 Glucose, 10 HEPES acid]. Arteries were cannulated at both ends onto micropipette tips (0.125 mm; DMT Systems, Aarhus, Denmark) in the chamber of a pressure myography system (110p; DMT Systems, Aarhus, Denmark). Following preincubation in 37 °C PSS for 1 hour, the outer vessel diameter was recorded using an inverted microscope with a video camera (TS100; Nikon Eclipse, Melville, NY), with data streamed in real time to edge detection software (DMT VAS version 0.2.0). Arteries were assessed for leakage and only those that did not leak were used to assess vasodilatory function. After pre-constriction with phenylephrine (PE, 10⁻⁹ to 10⁻³ M; Sigma, St. Louis, MO) to ~ 50 - 65% of the maximum PE response, the vasodilatory response to BuOE was assessed. Increasing doses of BuOE were added to the chamber to achieve final concentrations from 0.5 to 20 μM. Subsets of arteries were pretreated with an endothelial nitric oxide (•NO) synthase (NOS) inhibitor *NG-nitro-L-arginine methyl ester* (L-NAME, Sigma, St. Louis, MO; 0.1 M, 10 min) prior to the BuOE dose response.

Changes in vessel diameter are represented as percentage vasodilation from baseline and calculated using the following equation: $(D_{Dose} - D_p / D_1 - D_p) \times 100$, where D_{Dose} is the recorded diameter as consequence of a given treatment (i.e., drug dose), D_p is the diameter recorded after the addition of the vasoconstrictor (i.e., PE), and D_1 is the diameter recorded immediately before the addition of the vasoconstrictor (initial diameter).

Doppler imaging

To allow for clear imaging of the abdominal region, hair was removed from the mice using Nair one day prior to imaging, taking care not to burn the skin by using excess Nair or by leaving the Nair on too long. On the day of imaging, normotensive and AngII-hypertensive mice were anesthetized by isoflurane inhalation (1 2.5%) before being placed on a heated stage in a supine position. Mice were kept under anesthesia by isoflurane inhalation (1 2%) for the duration of the procedure.

The superior mesenteric artery (SMA) was selected for imaging due to its anatomical location which is routinely identifiable and allows for clear analysis of blood flow. Ultrasound gel was applied to the abdominal region and the SMA was located using a combination of B-mode and color Doppler on the high frequency Vevo 3100 [FujiFilm VisualSonics Inc ultrasound machine and a MX550D transducer (center frequency 40 MHz, axial resolution 100 μm) Toronto, Canada]. Blood velocity, reported as velocity time integral (VTI), was measured using pulse-wave Doppler with the doppler gate placed at the site of maximum velocity.

After obtaining baseline VTI of the SMA, BuOE (1 mg/kg, 100 μL) was administered IP and VTI measurements of the SMA were taken every 5 min for 30 min. VisualSonics VevoLab software (Toronto, Canada) was used for post-imaging analysis and measurements.

Statistical analysis

All data are expressed as mean ± standard error of the mean (SEM). Two-way ANOVA followed by Bonferroni Post-Hoc test were used to analyze the blood pressure measurements. Treatment indicates a difference between various treatment groups (vehicle and BuOE). Time indicates a difference over time. Interaction indicates whether the effect of treatment depends on the effect of time. For the renal sympathetic nerve recordings, data were analyzed by two-way ANOVA followed by

Bonferroni Post-Hoc test. EPR spectroscopy data were analyzed via Student's *t*-test. The myography data were analyzed via two-way ANOVA followed by Bonferroni Post-Hoc test. For the doppler imaging measurements, the data were analyzed via one-way ANOVA followed by Bonferroni Post-Hoc test. A *p*-value less than 0.05 was considered to be statistically significant. All statistical analyses were completed using Prism 8 (GraphPad Software Inc, San Diego, CA).

Results

BuOE acutely decreases hypertensive blood pressure in mice

The average baseline, normotensive SBP, DBP, and MAP, as indicated by the dashed line in Figs. 1 2, in all mice was 111 ± 1.2 mmHg, 81 ± 1.7 mmHg, and 97 ± 1.4 mmHg, respectively. To determine if BuOE decreases hypertensive blood pressure in AngII-induced hypertensive mice, blood pressure was monitored for two hours post-IP injection of BuOE (1 & 5 mg/kg) or vehicle (100 μL) into mice with established hypertensive blood pressures (MAP ~140 mmHg). Both 1 and 5 mg/kg BuOE significantly decreased SBP (Fig. 1A), DBP (Fig. 1B), and MAP (Fig. 1C) immediately following the IP injection. While both concentrations induced a significant hypotensive response and the blood pressures gradually return back to the hypertensive baseline, 5 mg/kg BuOE had a much longer hypotensive response (> 2 h) compared to 1 mg/kg BuOE (< 2 h).

Expanding upon these IP injections, systolic, diastolic and mean blood pressures were also monitored following IV injections of BuOE (0.1 1 mg/kg) or vehicle into AngII-hypertensive mice. BuOE induced a significant dose-dependent decrease in SBP (Fig. 2A), DBP (Fig. 2B), and MAP (Fig. 2C) immediately following the IV injection. Notably, 0.1 mg/kg BuOE induced a transient hypotensive response that lasted less than 30 min, while the higher concentrations of BuOE (0.5 & 1 mg/kg) had prolonged hypotensive responses lasting longer than 2 h before returning to hypertensive baseline values. Further, the IV-induced hypotensive response was more robust than observed after IP administration (Fig. 1).

Of note, vehicle-treated mice exhibit a slight increase in blood pressure immediately following the IP or IV injection (Figs. 1 & 2, respectively). This was due to handling the mice to perform the injection. Upon returning the animals to their home cage post-injection, the blood pressure returns to the hypertensive baseline values. Taken together, these data suggest that BuOE immediately and transiently decreases blood pressure in AngII-hypertensive mice.

BuOE transiently decreases RSNA and MAP followed by an increase in HR in WKY rats & SHR

To begin examining the mechanism(s) by which BuOE induces its hypotensive response, we investigated the effect of BuOE on the sympathetic nervous system, which is known to play a key role in blood pressure regulation [28]. Specifically, changes in RSNA, BP, and HR in anesthetized, normotensive WKY rats (Fig. 3A) and SHRs (Fig. 3B) were measured following injections (IV) of 0.05 mg/kg BuOE. As shown in Fig. 3C, BuOE significantly decreased RSNA in both WKYs and SHRs within ten seconds (immediate time point) before increasing above baseline. While RSNA in the WKYs dropped below baseline during subsequent time points, RSNA in SHRs remained above baseline. The immediate drop in RSNA was accompanied by a concomitant and significant decrease in MAP that gradually returned to baseline by 30 min post-injection for both WKY rats and SHRs (Fig. 3D). Following the immediate decreases in RSNA and MAP, HR increased for both WKY rats and SHRs (Fig. 3E). The increase in HR was mostly likely a reflex response to a drop in arterial pressure. Of note, RSNA, MAP and HR were not altered from baseline following IV injection vehicle (saline) (unpublished observations). Collectively, these results suggest that BuOE-induced sym-

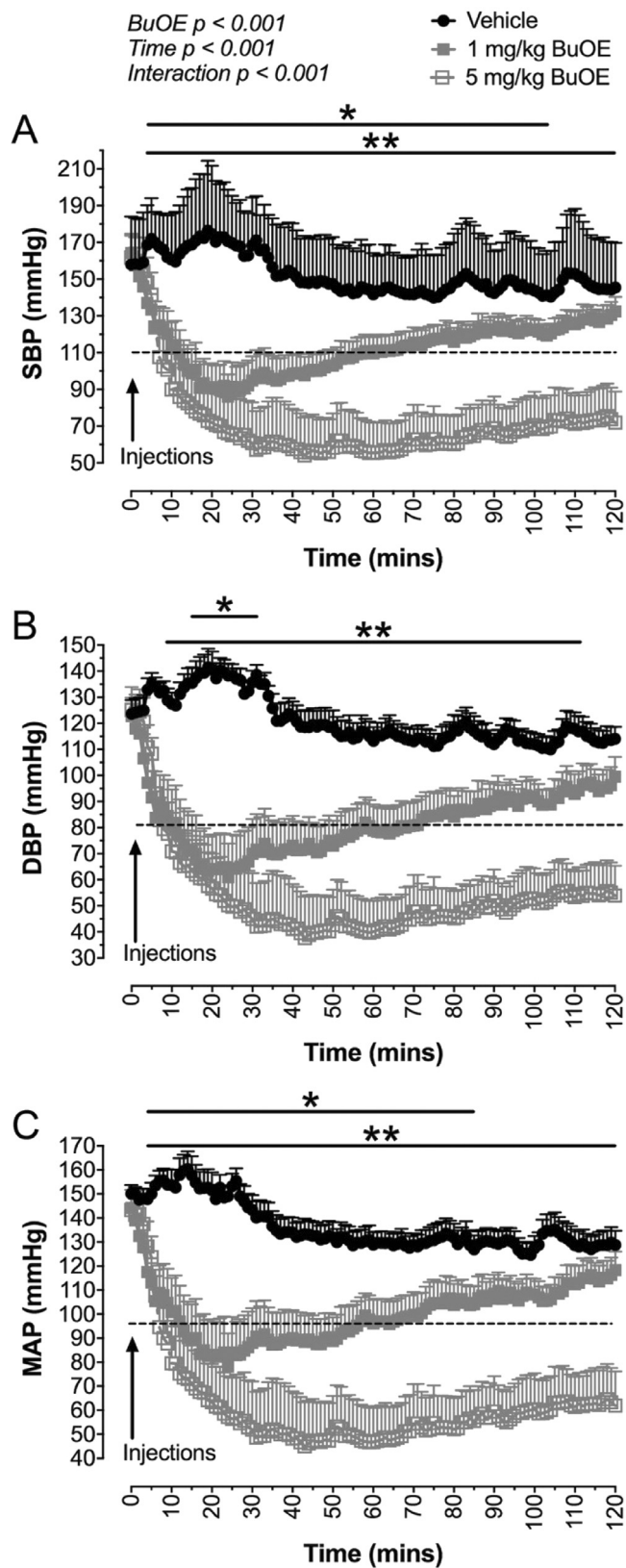


Fig. 1. BuOE administered intraperitoneally (IP) immediately and acutely decreases blood pressure in AngII-hypertensive mice. A: Systolic blood pressure (SBP), B: Diastolic blood pressure (DBP), and C: Mean arterial pressure (MAP) of mice given BuOE (1 or 5 mg/kg) or vehicle (saline) IP. Dashed line indicates pre-AngII baseline blood pressure. Data are displayed as means \pm SEM. * $p < 0.05$ vs 1 mg/kg BuOE, ** $p < 0.05$ vs 5 mg/kg BuOE (two-way ANOVA with Bonferroni post hoc test). $n = 10$ (1 mg/kg BuOE); 8 (5 mg/kg BuOE); 12 (Vehicle).

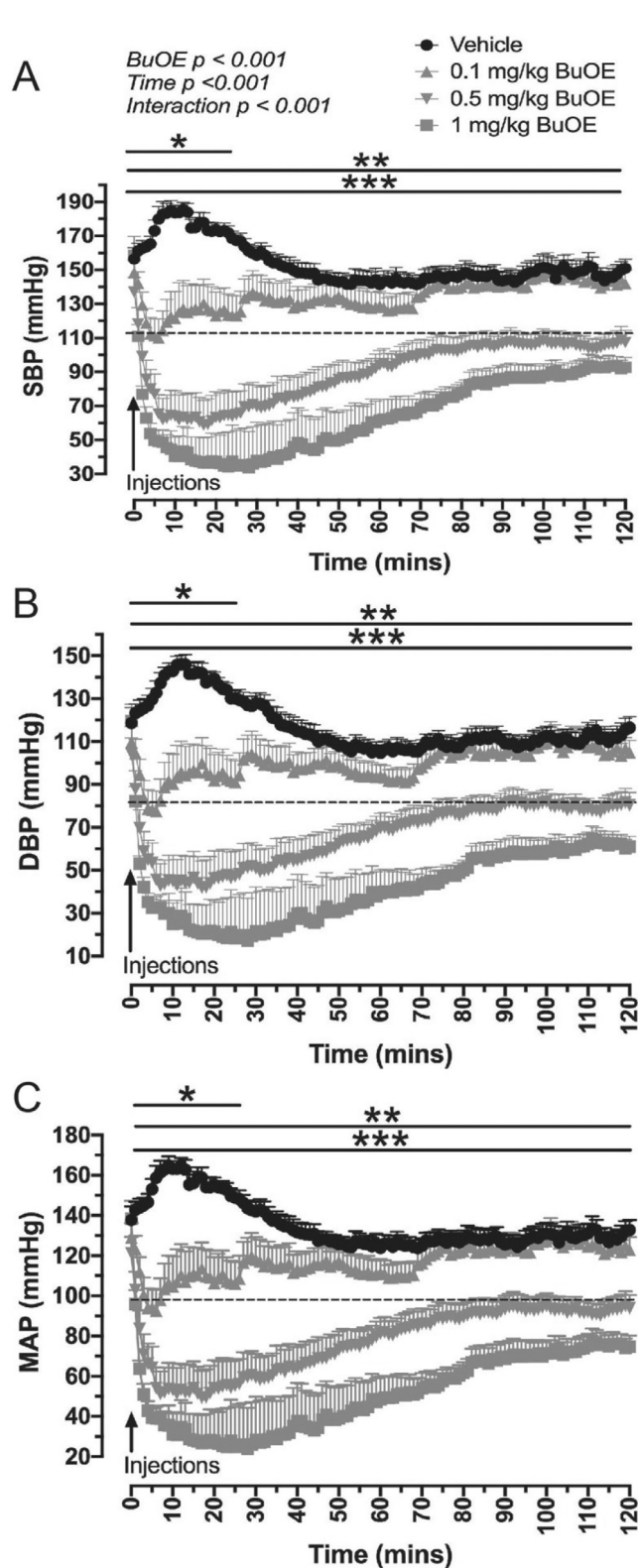


Fig. 2. BuOE administered intravenously (IV) immediately and acutely decreases blood pressure in AngII-hypertensive mice. A: Systolic blood pressure (SBP), B: Diastolic blood pressure (DBP), and C: Mean arterial pressure (MAP) of mice given BuOE (0.1 - 1 mg/kg) or vehicle (saline) IV. Dashed line indicates pre-AngII baseline blood pressure. Data are displayed as means \pm SEM. * $p < 0.05$ vs 0.1 mg/kg BuOE, ** $p < 0.05$ vs 0.5 mg/kg BuOE, *** $p < 0.05$ vs 1 mg/kg BuOE (two-way ANOVA with Bonferroni post hoc test). $n = 4$ (0.1 mg/kg BuOE); 5 (0.5 mg/kg BuOE); 3 (1 mg/kg BuOE); 14 (Vehicle).

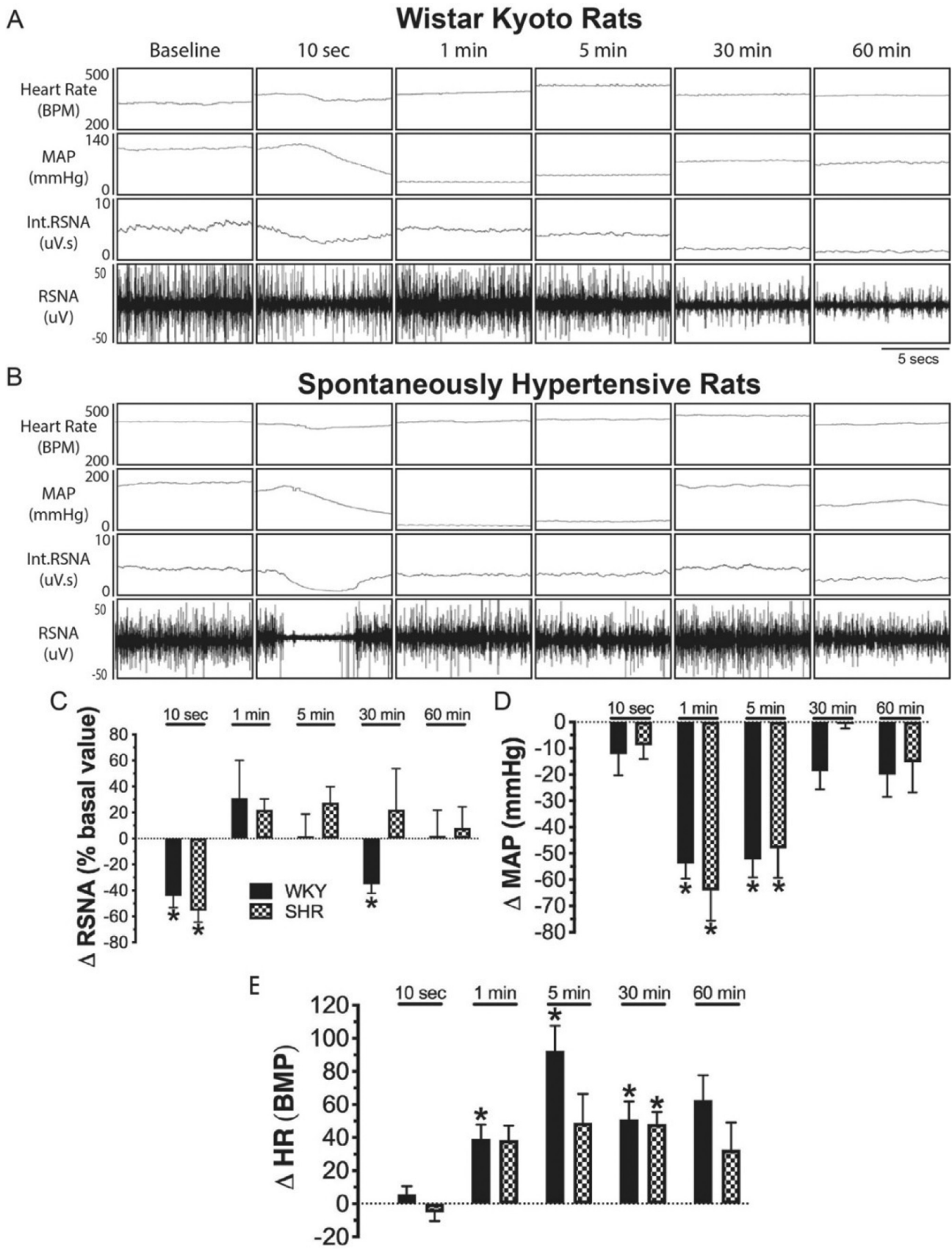


Fig. 3. BuOE transiently decreases renal sympathetic nerve activity (RSNA) and mean arterial pressure (MAP) in WKY and SHR rats. Representative tracings of heart rate (HR), MAP, integrated (Int) RSNA and raw RSNA in WKY (A) and SHR rats (B) injected with BuOE (0.05 mg/kg, IV) at baseline, 10 s, 1 min, 5 min, 30 min, and 60 min. C: Summary data showing change in RSNA as a percent of baseline. D: Summary data showing change in MAP from baseline. E: Summary data showing change in HR from baseline. Data are displayed as means \pm SEM. * p < 0.05 vs baseline (two-way ANOVA with Bonferroni post hoc test). n = 7 (WKY); 7 (SHR).

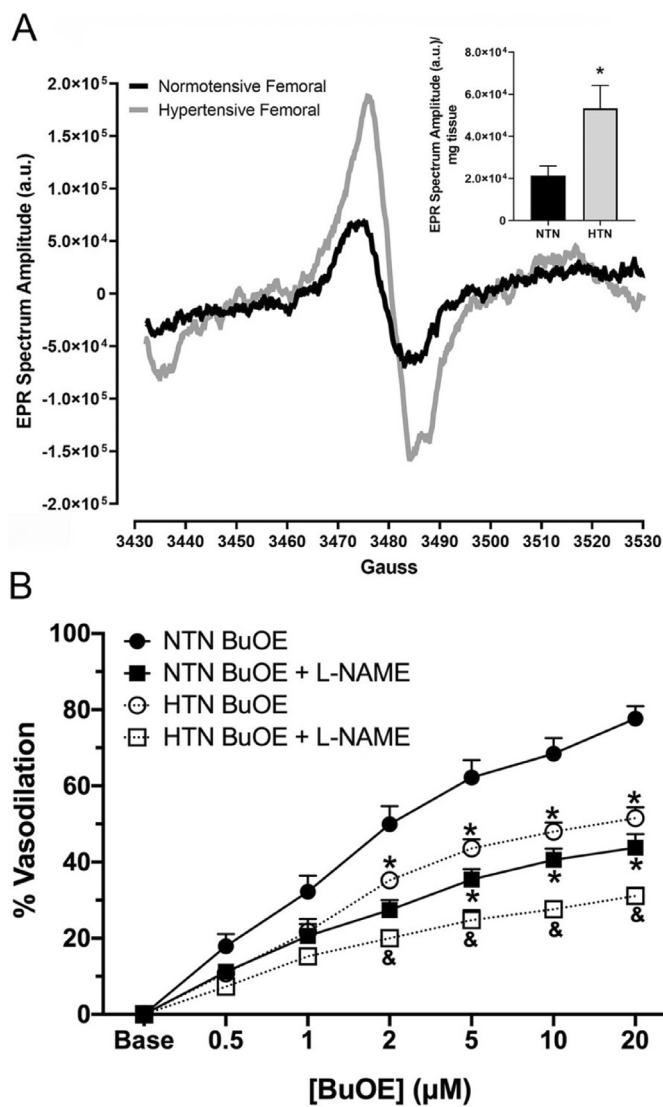


Fig. 4. BuOE induces vasodilation in a nitric oxide ($^{\bullet}\text{NO}$)-dependent manner. A) Representative CMH-EPR spectra obtained from femoral arteries isolated from normotensive (NTN) or AngII-hypertensive (HTN) mice. Inset: Summary EPR spectroscopy data showing $\text{O}_2^{\bullet-}$ levels in NTN and HTN femoral arteries, a.u. = arbitrary units. $^*p < 0.05$ vs NTN (Student's *t*-test). $n = 6$ (NTN); 7 (HTN). B) Isolated femoral arteries pre-constricted with phenylephrine were directly treated with BuOE and subjected to video myography. Subsets of arteries were pre-treated with L-NAME (0.1 M) prior to BuOE treatment. Data are displayed as means \pm SEM. $^*p < 0.05$ vs NTN BuOE, & $p < 0.05$ vs HTN BuOE (two-way ANOVA with Bonferroni post hoc test). $n = 10$ (NTN BuOE); 5 (NTN BuOE + L-NAME); 5 (HTN BuOE); 5 (HTN BuOE + L-NAME).

pathoinhibition contributes, at least in part, to BuOE's hypotensive response in normotensive and hypertensive rats.

BuOE induces vasodilation of normotensive and AngII-hypertensive mice vasculature

To determine the impact of BuOE on vascular reactivity, we first confirmed that $\text{O}_2^{\bullet-}$ levels are elevated in the vasculature from hypertensive mice compared to normotensive mice. Femoral arteries from normotensive and AngII-hypertensive mice were harvested, incubated with the $\text{O}_2^{\bullet-}$ -sensitive spin probe, CMH, and subject to EPR spectroscopy to detect $\text{O}_2^{\bullet-}$. The EPR spectra amplitudes (Fig. 4A) obtained from femoral vessels collected from AngII hypertensive mice were significantly greater than those obtained from normotensive mice, indicating

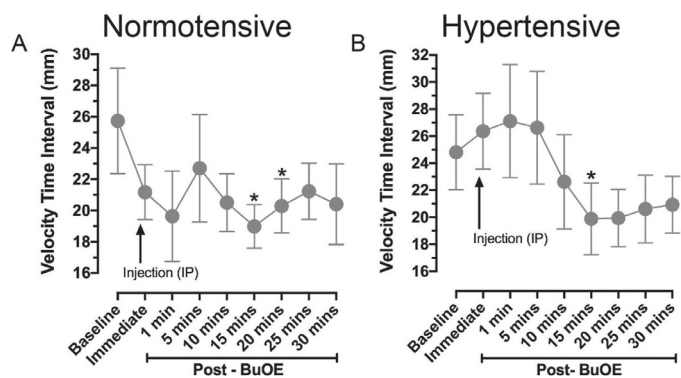


Fig. 5. BuOE decreases velocity time interval (VTI), indicative of vasodilation, in normotensive and AngII-hypertensive mice. Summary VTI collected from doppler imaging of the superior mesenteric artery (SMA) of A: normotensive and B: AngII-hypertensive mice given BuOE (1 mg/kg, IP). Data are displayed as means \pm SEM. $^*p < 0.05$ vs baseline (one-way ANOVA with Bonferroni post hoc test). $n = 5$ (normotensive); 5 (hypertensive).

an increase in $\text{O}_2^{\bullet-}$ in hypertensive vasculature, as previously reported by others [9, 29].

Next, we directly assessed reactivity of femoral arteries collected from AngII-hypertensive or normotensive mice using video myography. BuOE (0.5–20 μM) induced a significant dose-dependent increase in vasodilation of arteries from both normotensive and AngII-hypertensive mice (Fig. 4B). To investigate the role of $^{\bullet}\text{NO}$ in mediating BuOE-induced vasodilation, a subset of isolated arteries from normotensive and hypertensive mice were pre-treated with NOS inhibitor L-NAME (0.1 M). Inhibiting $^{\bullet}\text{NO}$ production via pretreatment with L-NAME significantly attenuated BuOE-induced vasodilation (Fig. 4). These data suggest that $^{\bullet}\text{NO}$ is mediating, at least in part, BuOE's vasodilatory response.

To expand upon the *ex vivo* myography data, doppler imaging was used to determine the impact of BuOE on vascular reactivity *in vivo*. The SMA of normotensive and AngII-hypertensive mice were imaged for 30 min following BuOE (1 mg/kg, IP) injection. Blood velocity, reported as velocity time integral (VTI), decreased over time (Fig. 5) with a significant decrease at 15 min post-injection. Since velocity is inversely related to cross sectional area of the vessel, a decrease in velocity is representative of vasodilation. Thus, taken together with the myography data, we conclude that BuOE induces vasodilation in normotensive and AngII-hypertensive mice.

Discussion

Extensive research over the last few decades has illuminated a vast amount of knowledge on the role of ROS, particularly $\text{O}_2^{\bullet-}$, in cardiovascular diseases such as heart failure and hypertension. In the pursuit of restoring physiological redox balance, numerous labs have investigated the role of exogenous SOD protein or SOD mimics as novel anti-hypertensive therapeutics. The present work focused on a manganese porphyrin SOD mimic, BuOE, and its effect on blood pressure in two different rodent models of hypertension, AngII-hypertensive mice and SHR. After confirming our hypothesis that BuOE decreases hypertensive blood pressures, we attempted to elucidate the mechanism(s) by which this hypotensive response occurs. We demonstrate that BuOE transiently inhibits sympathetic nerve activity and induces vasodilation, with the latter being attenuated by NOS inhibition. Taken together, our results indicate that sympathoinhibition and vasodilation contribute, at least in part, to the acute decrease in hypertensive blood pressure induced by the SOD mimic, BuOE.

Manganese porphyrins have been shown to be some of the most efficacious SOD mimics [18, 30] and have become a viable option for the treatment of various diseases with perturbed redox environments.

The positive charges on the manganese metal center as well as the constituents surrounding the porphyrin ring help attract $O_2^{\bullet-}$ [31]. The first of the porphyrin-based SOD mimics, T2E has been studied in numerous cancers as a radioprotector [32, 33]. However, it is limited by its hydrophilicity and does not cross the blood brain barrier (BBB). As a result, the constituting alkyl chains were lengthened resulting in MnTnHex-2-PyP⁵⁺ (MnHEX) [18, 30]. However, MnHEX was limited by its toxicity [34]. The insertion of oxygen into the alkyl chains decreased toxicity, while maintaining the enhanced lipophilicity and resulted in the generation of BuOE [16]. BuOE's ability to scavenge superoxide and induce cellular responses via oxidation/S-glutathionylation of proteins in the NF- κ B and Nrf2 signaling pathways [35, 36] has led to BuOE being clinically evaluated in numerous cancers [15]. The success of BuOE in cancer clinical trials has promoted the study of BuOE in other experimental disease models including diabetes, obesity, and cardiovascular diseases [18]. Anselmo et al. (2018) studied BuOE in AngII-induced mouse aortic valve remodeling and found that BuOE prevented thickening of the AV valve by preventing accumulation of extracellular matrix components [21]. Previous work in our lab has shown that BuOE decreases normotensive blood pressure via sympathoinhibition [19].

The present work builds upon our previous studies by demonstrating that BuOE decreases hypertensive blood pressures when administered either IP or IV. When given IP (Fig. 1), 5 mg/kg BuOE induced a greater hypotensive response (~ -100 mmHg) than 1 mg/kg BuOE (~ -60 mmHg). Additionally, the higher 5 mg/kg BuOE response was maintained for a longer period of time (beyond two hours), whereas 1 mg/kg BuOE returned to baseline levels by the end of the two-hour recording. BuOE (1 mg/kg) given IV (Fig. 2) had a similar response to 5 mg/kg BuOE given IP with a decrease in blood pressure of approximately 100 mmHg and a prolonged response that remained significantly decreased for at least two hours. A similar response was seen with 0.5 mg/kg BuOE given IV. However, the lowest concentrations of BuOE (0.1 mg/kg) given IV had the most transient decrease in blood pressure (~ -40 mmHg), lasting only approximately 30 min. These data indicate that BuOE's blood pressure effect is concentration dependent. The location of BuOE also appears to alter its blood pressure effects, as having a large bolus amount in the vasculature (i.e., IV administration) results in more robust changes in blood pressure. In comparison to our previous work in normotensive mice, BuOE also induced a more robust decrease in hypertensive mice. For example, 1 mg/kg BuOE (IP) decreased MAP by approximately 30 mmHg [19] in normotensive mice, whereas the same concentration and route of administration of BuOE in hypertensive animals decrease MAP by approximately 60 mmHg (Fig. 1). In fact, for all of the various concentrations and routes of administration tested in this work, BuOE induced a more robust decrease in MAP in AngII-hypertensive mice than in normotensive mice. This work matches hemodynamic work in anesthetized rats treated with T2E (IV) [37], the BuOE-induced hypotensive response seen in dogs [20], as well as the side effects of the highest dose of BuOE given as a radioprotector to cancer patients in clinical trials (unpublished data).

While much lower doses of BuOE appear to be efficacious in preventing radiation damage in cancer patients receiving radiation therapy [15], determining the mechanism(s) by which BuOE induces its hypotensive response may provide new insights that allow for further enhancement of BuOE's safety profile in clinical trials as well as the potential for a novel anti-hypertensive therapeutic. As such, we investigated BuOE's effect on the sympathetic nervous system and the vasculature, two key components of physiological and pathophysiological blood pressure regulation.

Numerous studies have shown the contribution of $O_2^{\bullet-}$ to the enhanced sympathoexcitation contributing to cardiovascular diseases such as heart failure and hypertension [7, 38–40]. Specifically, elevated $O_2^{\bullet-}$ in specific brain nuclei, such as the rostral ventral lateral medulla (RVLM) which are known to regulate sympathetic drive and influence blood pressure regulation, contribute to hypertensive blood pressures [7, 38]. Scavenging $O_2^{\bullet-}$ in these brain regions attenuates hypertension

[7, 14, 41, 42]. Thus, using anesthetized SHR and their normotensive control WKY rats, we recorded RSNA to evaluate the contribution of the sympathetic nervous system to BuOE's hypotensive response (Fig. 3). For both WKY rats and SHRs, RSNA significantly decreased immediately (within 10 secs) after BuOE (0.05 mg/kg, IV) injection. We suspect that BuOE is crossing the BBB, where it scavenges $O_2^{\bullet-}$ in cardiovascular control brain nuclei, like the RVLM, resulting in this sympathoinhibition. Notably, biodistribution studies have shown that BuOE can cross the BBB and accumulate in various areas of the brain including the cortex, thalamus, and brainstem [17, 43, 44]. Importantly, the brainstem contains critical cardiovascular control nuclei, such as the RVLM. However, to date, pharmacokinetics and biodistribution studies of BuOE have not investigated acute timepoints (i.e., seconds to minutes). Therefore, it remains unknown if the immediate decrease in RSNA observed in our study is due to BuOE crossing the BBB and impacting neuronal activity in the RVLM. An alternative interpretation of our RSNA data is that BuOE attenuates afferent nerve activity from the kidney to the brain leading to the observed sympathoinhibition. In our RSN recording preparation, we measure both efferent and afferent nerve activity together. Further investigation is required to elucidate BuOE's impact on efferent versus afferent RSNA.

Following the immediate decrease in RSNA, there was a return to baseline (1 min) before dropping below baseline for the rest of the recording in normotensive WKY rats. This return to baseline was concomitant with MAP returning to baseline levels. In contrast, in SHRs, RSNA returned to baseline and remained above baseline for the duration of the recording. We postulate that the prolonged increase in RSNA in SHRs is the result of overcompensation for the decrease in blood pressure and overactivation of the baroreflex. The increase in HR in the SHRs at 1 min and beyond post-BuOE injection is consistent with an enhanced overall sympathoexcitation and is in agreement with increased RSNA at those timepoints. Furthermore, this increase in HR is congruent with the non-clinical safety and toxicity studies that showed an increase in HR in non-human primates following BuOE administration [20]. Additionally, the immediate decrease in RSNA and BP as well as an increase in HR are consistent with our previous work using normotensive Sprague Dawley rats [19].

Another key component of blood pressure regulation is the vasculature. Increased $O_2^{\bullet-}$ levels in the vasculature (Fig. 4A) have been reported in hypertensive animal models [9, 29] and linked to endothelial dysfunction as well as impaired vascular reactivity [9]. Moreover, $O_2^{\bullet-}$ reacts with \bullet NO, a key vasodilator, at a diffusion-limited rate resulting in reduced bioavailability of \bullet NO and vasoconstriction. We investigated the effects of BuOE on vascular reactivity *ex vivo* via myography and *in vivo* via doppler imaging. Our myography study shows that BuOE significantly vasodilates isolated skeletal muscle arteries collected from both normotensive and AngII-hypertensive mice in a dose-dependent manner (Fig. 4B). We postulate that BuOE is scavenging $O_2^{\bullet-}$ in the vasculature, increasing \bullet NO bioavailability, which results in vasodilation. The \bullet NO-dependent vasodilation is supported by the fact that pretreatment with L-NAME, an eNOS inhibitor, significantly attenuates BuOE-induced vasodilation. Of note, the impact of \bullet NO may extend beyond the vasculature. \bullet NO in cardiovascular control brain nuclei is known to induce sympathoinhibition [45, 46]. We speculate that BuOE's scavenging of $O_2^{\bullet-}$ in the brain increases \bullet NO bioavailability, thereby leading to the sympathoinhibition we observed (Fig. 3). Future studies are needed to investigate this potential mechanism.

Interestingly, inhibition of \bullet NO via L-NAME did not completely abolish the BuOE-induced vasodilation (Fig. 4B), indicating an additional mechanism(s) may be playing a role in BuOE's vasodilatory response. Another ROS, hydrogen peroxide (H_2O_2) has been linked to vasodilation [47] and is formed from the dismutation of $O_2^{\bullet-}$. As such, H_2O_2 could be responsible for BuOE's \bullet NO-independent vasodilation. Additionally, calcium is known to play a role in the regulation of vascular tone [48, 49] via increased $O_2^{\bullet-}$. In fact, another manganese porphyrin, MnTBAP has been shown to inhibit calcium ionophore A23187-induced

increase in ROS via both scavenging ROS and modulation of calcium channels [50–52]. Additionally, T2E has been shown to increase calcium transients and increase sarcoplasmic reticulum calcium load in a rat model of arrhythmias [53]. Thus, it is possible that \bullet NO-independent BuOE-induced vasodilation could be the result of a calcium-dependent mechanism. Further, considering the importance of redox mechanisms and the flow of electrons through eNOS for its activity, it is possible the BuOE has direct effects on the activity the enzyme. Ongoing studies in our laboratory are currently testing these hypotheses.

We sought to extend our myography data in vivo using doppler imaging of the SMA. BuOE (1 mg/kg, IP) decreased VTI in normotensive and AngII-hypertensive mice (Fig. 5) over time. VTI is representative of blood velocity. Since velocity is inversely related to cross sectional area of a vessel, a decrease in velocity is indicative of vasodilation, thereby confirming the *ex vivo* myography results. Furthermore, the significant vasodilation at 15–20 min post BuOE-injection is in agreement with the peak response of BuOE at the same dose and route of administration (1 mg/kg, IP) given to normotensive animals [19] and hypertensive animals (Fig. 1). This is also in agreement with other work demonstrating that BuOE prevented acute vasoocclusion and reestablished blood flow in a mouse model of sickle cell disease [54, 55].

In conclusion, we have demonstrated that BuOE acutely decreases blood pressure in hypertensive animal models via inhibition of the sympathetic nervous system and vasodilation. These results are crucial to not only enhancing the safety for patients in clinical trials receiving BuOE as a radioprotector but may provide a novel-anti-hypertensive therapeutic option for the many Americans who struggle to control their hypertension. Therefore, future chronic hypertensive studies are needed to investigate the long-term impact of BuOE on elevated blood pressure.

Disclosures

The authors declare the following financial interests/personal relationships which may be considered as potential competing interests: Dr. Oberley-Deegan is a consultant with BioMimetix Pharmaceutical, Inc. and holds equities in BioMimetix Pharmaceutical, Inc. There are no other conflicts of interest reported by the authors.

Declaration of Competing Interest

The authors declare that they have no known competing financial interests or personal relationships that could have appeared to influence the work reported in this paper.

CRedit authorship contribution statement

Sarah L. Schlichte: Investigation, Methodology, Data curation, Formal analysis, Supervision, Resources, Writing – original draft, Writing – review & editing. **Elizabeth J. Pekas:** Investigation, Data curation, Formal analysis, Writing – review & editing. **Taylor J. Bruett:** Investigation, Writing – review & editing. **Bryan T. Hackfort:** Investigation, Writing – review & editing. **Jordan M. Rasmussen:** Investigation, Data curation, Formal analysis, Writing – review & editing. **Kaushik P. Patel:** Investigation, Methodology, Supervision, Writing – review & editing. **Song-Young Park:** Investigation, Data curation, Formal analysis, Writing – review & editing. **Rebecca E. Oberley-Deegan:** Investigation, Methodology, Supervision, Writing – review & editing. **Matthew C. Zimmerman:** Investigation, Methodology, Supervision, Writing – review & editing.

Acknowledgements

This project was supported, in part, by the UNMC Center for Heart and Vascular Research (CHVR) and by the National Institutes of Health (NIH) National Institute of General Medical Sciences, 1U54GM115458, which funds the Great Plains IDEa-CTR Network. The content is solely

the responsibility of the authors and does not necessarily represent the official views of CHVR or the NIH. This work was also supported by a NIH predoctoral fellowship (F31HL152580; to S.L. Schlichte). We also acknowledge support from the NIH Center of Biomedical Research Excellence (COBRE) grant awarded to the UNMC's Nebraska Center for Nanomedicine (P30GM127200). EPR spectroscopy data was collected in the University of Nebraska's EPR Spectroscopy Core, which was initially established with support from a Center of Biomedical Research Excellence grant from the National Institute of General Medical Sciences of the National Institutes of Health (P30-GM103335) awarded to the University of Nebraska's Redox Biology Center. Additional support came from the Center for Research in Human Movement Variability, NIH P20 GM109090; (to S.Y. Park), NIH R01 CA178888; (to R.E. Oberley-Deegan), NIH R01 DK114663, P01 HL62222, and endowed McIntyre Professorship fund; (to K.P. Patel).

References

- [1] Facts About Hypertension | cdc.gov [Online]. [date unknown]. <https://www.cdc.gov/bloodpressure/facts.htm> [19 May 2021].
- [2] Hypertension [Online]. [date unknown]. <https://www.who.int/news-room/factsheets/detail/hypertension>, 19 May 2021.
- [3] D.G. Harrison, M.C. Gongora, T.J. Guzik, J. Widder, Oxidative stress and hypertension, *J. Am. Soc. Hypertens.*, 1 (2007) 30–44, doi:10.1016/j.jash.2006.11.006.
- [4] R. Loperena, D.G. Harrison, Oxidative stress and hypertensive diseases, *Med. Clin. North Am.* 101 (2017) 169–193, doi:10.1016/j.mcna.2016.08.004.
- [5] K.K. Griendling, L.L. Camargo, F.J. Rios, R. Alves-Lopes, A.C. Montezano, R.M. Touyz, Oxidative stress and hypertension, *Circ. Res.*, 128 (2021) 993–1020, doi:10.1161/CIRCRESAHA.121.318063.
- [6] M.C. Zimmerman, E. Lazartigues, J.A. Lang, P. Sinnayah, I.M. Ahmad, D.R. Spitz, R.L. Davisson, Superoxide mediates the actions of angiotensin II in the central nervous system, *Circ. Res.* 91 (2002) 1038–1045, doi:10.1161/01.RES.0000043501.47934.FA.
- [7] M.-H. Tai, Li-L. Wang, K.L.H. Wu, J.Y.H. Chan, Increased superoxide anion in rostral ventrolateral medulla contributes to hypertension in spontaneously hypertensive rats via interactions with nitric oxide, *Free Radic. Biol. Med.* 38 (2005) 450–462, doi:10.1016/j.freeradbiomed.2004.11.015.
- [8] L. Kopkan, A. Castillo, L.G. Navar, D.S.A. Majid, Enhanced superoxide generation modulates renal function in ANG II-induced hypertensive rats, *Am. J. Physiol. Renal Physiol.*, 290 (2006) F80–F86, doi:10.1152/ajprenal.00090.2005.
- [9] R.M. Touyz, Reactive oxygen species, vascular oxidative stress, and redox signaling in hypertension: what is the clinical significance? *Hypertension* 44 (2004) 248–252, doi:10.1161/01.HYP.0000138070.47616.9d.
- [10] R. Rodrigo, J. González, F. Paoletto, The role of oxidative stress in the pathophysiology of hypertension, *Hypertens. Res.*, 34 (2011) 431–440, doi:10.1038/hr.2010.264.
- [11] H. Xu, G.D. Fink, J.J. Galligan, Tempol lowers blood pressure and sympathetic nerve activity but not vascular O₂⁻ in DOCA-salt rats, *Hypertension* 43 (2004) 329–334, doi:10.1161/01.HYP.0000112304.26158.5c.
- [12] E.G. Rosenbaugh, J.W. Roat, L. Gao, R.-F. Yang, D.S. Manickam, J.-X. Yin, H.D. Schultz, T.K. Bronich, E.V. Batrakova, A.V. Kabanov, I.H. Zucker, M.C. Zimmerman, The attenuation of central angiotensin II-dependent pressor response and intra-neuronal signaling by intracarotid injection of nanoformulated copper/zinc superoxide dismutase, *Biomaterials* 31 (2010) 5218–5226, doi:10.1016/j.biomaterials.2010.03.026.
- [13] K. Savalia, D.S. Manickam, E.G. Rosenbaugh, J. Tian, I.M. Ahmad, A.V. Kabanov, M.C. Zimmerman, Neuronal uptake of nanoformulated superoxide dismutase and attenuation of angiotensin II-dependent hypertension after central administration, *Free Radic. Biol. Med.* 73 (2014) 299–307, doi:10.1016/j.freeradbiomed.2014.06.001.
- [14] J.P. Collister, H. Taylor-Smith, D. Drebes, D. Nahey, J. Tian, M.C. Zimmerman, Angiotensin II-Induced hypertension is attenuated by overexpressing copper/zinc superoxide dismutase in the brain organum vasculosum of the lamina terminalis, *Oxid. Med. Cell. Longev.* 2016 (2016) 1–9, doi:10.1155/2016/3959087.
- [15] Search of BMX-001 - List Results - ClinicalTrials.gov [Online]. [date unknown]. <https://clinicaltrials.gov/ct2/results?cond=&term=BMX-001&cntry=&state=&city=&dist=>, 20 Apr. 2020.
- [16] Z. Rajic, A. Tovmasyan, I. Spasojevic, H. Sheng, M. Lu, A.M. Li, E.B. Gralla, D.S. Warner, L. Benov, I. Batinic-Haberle, A new SOD mimic, Mn(III) ortho N-butoxyethylpyridylporphyrin, combines superb potency and lipophilicity with low toxicity, *Free Radic. Biol. Med.* 52 (2012) 1828–1834, doi:10.1016/j.freeradbiomed.2012.02.006.
- [17] D. Leu, I. Spasojevic, H. Nguyen, B. Deng, A. Tovmasyan, T. Weitner, R.S. Sampaio, I. Batinic-Haberle, T.-T. Huang, CNS bioavailability and radiation protection of normal hippocampal neurogenesis by a lipophilic Mn porphyrin-based superoxide dismutase mimic, MnTnBuOE-2-PyP5+, *Redox Biol.*, 12 (2017) 864–871, doi:10.1016/j.redox.2017.04.027.
- [18] I. Batinic-Haberle, A. Tovmasyan, I. Spasojevic, Mn porphyrin-based redox-active drugs: differential effects as cancer therapeutics and protectors of normal tissue against oxidative injury, *Antioxid. Redox Signal.* 29 (2018) 1691–1724, doi:10.1089/ars.2017.7453.

- [19] S.L. Schlichte, S. Romanova, K. Katsurada, E.A. Kosmacek, T.K. Bronich, K.P. Patel, R.E. Oberley-Deegan, M.C. Zimmerman, Nanoformulation of the superoxide dismutase mimic, MnTnBuOE-2-PyP⁵⁺, prevents its acute hypotensive response, *Redox Biol.*, 36 (2020) 101610, doi:10.1016/j.redox.2020.101610.
- [20] S.C. Gad, D.W. Sullivan, I. Spasojevic, C.V. Mujer, C.B. Spainhour, J.D. Crapo, Non-clinical safety and toxicokinetics of MnTnBuOE-2-PyP⁵⁺ (BMX-001), *Int. J. Toxicol.*, 35 (2016) 438–453, doi:10.1177/1091581816642766.
- [21] W. Anselmo, E. Branchetti, J.B. Grau, G. Li, S. Ayoub, E.K. Lai, N. Rioux, A. Tovmasyan, J.H. Fortier, M.S. Sacks, I. Batinic-Haberle, S.L. Hazen, R.J. Levy, G. Ferrari, Porphyrin-based SOD mimic MnTnBuOE-2-PyP⁵⁺ inhibits mechanisms of aortic valve remodeling in human and murine models of aortic valve sclerosis, *J. Am. Heart Assoc.*, 7 (2018), doi:10.1161/JAHA.117.007861.
- [22] U. Basu, A.J. Case, J. Liu, J. Tian, Y.-L. Li, M.C. Zimmerman, Redox-sensitive calcium/calmodulin-dependent protein kinase II α in angiotensin II intra-neuronal signaling and hypertension, *Redox Biol.*, 27 (2019) 101230, doi:10.1016/j.redox.2019.101230.
- [23] A.J. Case, S. Li, U. Basu, J. Tian, M.C. Zimmerman, Mitochondrial-localized NADPH oxidase 4 is a source of superoxide in angiotensin II-stimulated neurons, *Am. J. Physiol. Heart Circ. Physiol.* 305 (2013) H19–H28, doi:10.1152/ajpheart.00974.2012.
- [24] H. Zheng, X. Liu, Y. Li, K.P. Patel, A hypothalamic leptin-glutamate interaction in the regulation of sympathetic nerve activity, *Neural Plast.* 2017 (2017) 1–11, doi:10.1155/2017/2361675.
- [25] N.M. Sharma, A.S. Haibara, K. Katsurada, X. Liu, K.P. Patel, Central angiotensin II-Protein inhibitor of neuronal nitric oxide synthase (PIN) axis contribute to neurogenic hypertension, *Nitric Oxide* 94 (2020) 54–62, doi:10.1016/j.niox.2019.10.007.
- [26] S.-Y. Park, S.J. Ives, J.R. Gifford, R.H.I. Andtbacka, J.R. Hyngstrom, V. Reese, G. Layec, L.P. Bharath, J.D. Symons, R.S. Richardson, Impact of age on the vasodilatory function of human skeletal muscle feed arteries, *Am. J. Physiol. Heart Circ. Physiol.*, 310 (2016) H217–H225, doi:10.1152/ajpheart.00716.2015.
- [27] S.-Y. Park, O.S. Kwon, R.H.I. Andtbacka, J.R. Hyngstrom, V. Reese, M.P. Murphy, R.S. Richardson, Age-related endothelial dysfunction in human skeletal muscle feed arteries: the role of free radicals derived from mitochondria in the vasculature, *Acta Physiol. (Oxf)* 222 (2018), doi:10.1111/apha.12893.
- [28] C.J. Barrett, Renal sympathetic nerves - what have they got to do with cardiovascular disease?: renal sympathetic nerves and cardiovascular disease, *Exp. Physiol.*, 100 (2015) 359–365, doi:10.1113/expphysiol.2014.080176.
- [29] R.M. Touyz, A.M. Briones, Reactive oxygen species and vascular biology: implications in human hypertension, *Hypertens. Res.*, 34 (2011) 5–14, doi:10.1038/hr.2010.201.
- [30] I. Batinic-Haberle, A. Tovmasyan, I. Spasojevic, An educational overview of the chemistry, biochemistry and therapeutic aspects of Mn porphyrins - From superoxide dismutation to H₂O₂-driven pathways, *Redox Biol.*, 5 (2015) 43–65, doi:10.1016/j.redox.2015.01.017.
- [31] A. Tovmasyan, H. Sheng, T. Weitner, A. Arulpragasam, M. Lu, D.S. Warner, Z. Vujaskovic, I. Spasojevic, Batinic-Haberle I. Design, Mechanism of action, bioavailability and therapeutic effects of mn porphyrin-based redox modulators, *Med. Princ. Pract.*, 22 (2013) 103–130, doi:10.1159/000341715.
- [32] A. Chatterjee, Y. Zhu, Q. Tong, E. Kosmacek, E. Lichter, R. Oberley-Deegan, The addition of manganese porphyrins during radiation inhibits prostate cancer growth and simultaneously protects normal prostate tissue from radiation damage, *Antioxidants* 7 (21) (2018), doi:10.3390/antiox7010021.
- [33] S. Shrishrimal, E. Kosmacek, A. Chatterjee, M. Tyson, Oberley-Deegan R. The SOD Mimic, MnTE-2-PyP, protects from chronic fibrosis and inflammation in irradiated normal pelvic tissues, *Antioxidants* 6 (2017) 87, doi:10.3390/antiox6040087.
- [34] B. Gauter-Fleckenstein, K. Fleckenstein, K. Owzar, C. Jiang, I. Batinic-Haberle, Z. Vujaskovic, Comparison of two Mn porphyrin-based mimics of superoxide dismutase in pulmonary radioprotection, *Free Radic. Biol. Med.* 44 (2008) 982–989, doi:10.1016/j.freeradbiomed.2007.10.058.
- [35] Y. Zhao, D.W. Carroll, Y. You, L. Chaiswing, R. Wen, I. Batinic-Haberle, S. Bondada, Y. Liang, D.K. St. Clair, A novel redox regulator, MnTnBuOE-2-PyP⁵⁺, enhances normal hematopoietic stem/progenitor cell function, *Redox Biol.*, 12 (2017) 129–138, doi:10.1016/j.redox.2017.02.005.
- [36] I. Batinic-Haberle, A. Tovmasyan, Z. Huang, W. Duan, L. Du, S. Siamakpour-Reihani, Z. Cao, H. Sheng, I. Spasojevic, A. Alvarez Secord, H₂O₂-driven anticancer activity of mn porphyrins and the underlying molecular pathways, *Oxid. Med. Cell. Longev.*, 2021 (2021) 1–23, doi:10.1155/2021/6653790.
- [37] A.D. Ross, H. Sheng, D.S. Warner, C.A. Piantadosi, I. Batinic-Haberle, B.J. Day, J.D. Crapo, Hemodynamic effects of metalloporphyrin catalytic antioxidants: structure-activity relationships and species specificity, *Free Radic. Biol. Med.* 33 (2002) 1657–1669, doi:10.1016/S0891-5849(02)01140-1.
- [38] S.H.H. Chan, K.-S. Hsu, C.-C. Huang, L.-L. Wang, C.-C. Ou, J.Y.H. Chan, NADPH oxidase-derived superoxide anion mediates angiotensin II-induced pressor effect via activation of p38 mitogen-activated protein kinase in the rostral ventrolateral medulla, *Circ. Res.* 97 (2005) 772–780, doi:10.1161/01.RES.0000185804.79157.CO.
- [39] L. Gao, W. Wang, Y.-L. Li, H.D. Schultz, D. Liu, K.G. Cornish, I.H. Zucker, Superoxide mediates sympathoexcitation in heart failure: roles of angiotensin II and NAD(P)H oxidase, *Circ. Res.* 95 (2004) 937–944, doi:10.1161/01.RES.0000146676.04359.64.
- [40] T.E. Lindley, M.F. Doobay, R.V. Sharma, R.L. Davison, Superoxide is involved in the central nervous system activation and sympathoexcitation of myocardial infarction-induced heart failure, *Circ. Res.* 94 (2004) 402–409, doi:10.1161/01.RES.0000112964.40701.93.
- [41] T. Kishi, Y. Hirooka, Y. Kimura, K. Ito, H. Shimokawa, A. Takeshita, Increased reactive oxygen species in rostral ventrolateral medulla contribute to neural mechanisms of hypertension in stroke-prone spontaneously hypertensive rats, *Circulation* 109 (2004) 2357–2362, doi:10.1161/01.CIR.0000128695.49900.12.
- [42] J. Collister, M. Bellrichard, D. Drebes, D. Nahey, J. Tian, M. Zimmerman, Overexpression of copper/zinc superoxide dismutase in the median preoptic nucleus attenuates chronic angiotensin II-induced hypertension in the rat, *IJMS* 15 (2014) 22203–22213, doi:10.3390/ijms151222203.
- [43] D.H. Weitzel, A. Tovmasyan, K.A. Ashcraft, Z. Rajic, T. Weitner, C. Liu, W. Li, A.F. Buckley, M.R. Prasad, K.H. Young, R.M. Rodriguez, W.C. Wetsel, K.B. Peters, I. Spasojevic, J.E. Herndon, I. Batinic-Haberle, M.W. Dewhirst, Radioprotection of the brain white matter by Mn(III) n-butoxyethylpyridylporphyrin-based superoxide dismutase mimic MnTnBuOE-2-PyP⁵⁺, *Mol. Cancer Ther.* 14 (2015) 70–79, doi:10.1158/1535-7163.MCT-14-0343.
- [44] D.H. Weitzel, A. Tovmasyan, K.A. Ashcraft, A. Boico, S.R. Birer, K. Roy Choudhury, J. Herndon, R.M. Rodriguez, W.C. Wetsel, K.B. Peters, I. Spasojevic, I. Batinic-Haberle, M.W. Dewhirst, Neurobehavioral radiation mitigation to standard brain cancer therapy regimens by Mn(III) n-butoxyethylpyridylporphyrin-based redox modifier: brain radiation mitigation by MnTnBuOE-2-PyP⁵⁺, *Environ. Mol. Mutagen.* 57 (2016) 372–381, doi:10.1002/em.22021.
- [45] K.P. Patel, Y.-F. Li, Y. Hirooka, Role of nitric oxide in central sympathetic outflow, *Exp. Biol. Med.* (Maywood) 226 (2001) 814–824, doi:10.1177/15353702012260902.
- [46] Z.-L. Guo, S.C. Tjen-A-Looi, L.-W. Fu, J.C. Longhurst, Nitric oxide in rostral ventrolateral medulla regulates cardiac-sympathetic reflexes: role of synthase isoforms, *Am. J. Physiol. Heart Circ. Physiol.* 297 (2009) H1478–H1486, doi:10.1152/ajp-heart.00209.2009.
- [47] R. Bretón-Romero, S. Lamas, Hydrogen peroxide signaling in vascular endothelial cells, *Redox Biol.*, 2 (2014) 529–534, doi:10.1016/j.redox.2014.02.005.
- [48] R.M. Touyz, Reactive oxygen species as mediators of calcium signaling by angiotensin II: implications in vascular physiology and pathophysiology, *Antioxid. Redox Signal.* 7 (2005) 1302–1314, doi:10.1089/ars.2005.7.1302.
- [49] R. Alves-Lopes, K.B. Neves, A. Anagnostopoulou, F.J. Rios, S. Lacchini, A.C. Montezano, R.M. Touyz, Crosstalk between vascular redox and calcium signaling in hypertension involves trpm2 (transient receptor potential melastatin 2) cation channel, *Hypertension* 75 (2020) 139–149, doi:10.1161/HYPERTENSIONAHA.119.13861.
- [50] Å. Petersén, R.F. Castilho, O. Hansson, T. Wielock, P. Brundin, Oxidative stress, mitochondrial permeability transition and activation of caspases in calcium ionophore A23187-induced death of cultured striatal neurons, *Brain Res.* 857 (2000) 20–29, doi:10.1016/S0006-8993(99)02320-3.
- [51] M. Aarts, K. Iihara, W.-L. Wei, Z.-G. Xiong, M. Arundine, W. Cerwinski, J.F. Macdonald, M. Tymianski, A key role for trpm7 channels in anoxic neuronal death, *Cell* 115 (2003) 863–877, doi:10.1016/S0092-8674(03)01017-1.
- [52] J.S. Tauskela, E. Brunette, L. Kiedrowski, K. Lortie, M. Hewitt, P. Morley, Unconventional neuroprotection against Ca²⁺-dependent insults by metalloporphyrin catalytic antioxidants, *J. Neurochem.*, 98 (2006) 1324–1342, doi:10.1111/j.1471-4159.2006.03973.x.
- [53] A.M. Barbosa, J.F. Sarmento-Neto, J.E.R. Menezes Filho, I.C.G. Jesus, D.S. Souza, V.M.N. Vasconcelos, F.D.L. Gomes, A. Lara, J.S.S. Araújo, S.S. Mattos, C.M.L. Vasconcelos, S. Guatimosim, J.S. Cruz, I. Batinic-Haberle, D.A.M. Araújo, J.S. Rebouças, E.R. Gomes, Redox-active drug, MnTE-2-PyP⁵⁺, prevents and treats cardiac arrhythmias preserving heart contractile function, *Oxid. Med. Cell. Longev.*, 2020 (2020) 1–15, doi:10.1155/2020/4850697.
- [54] A. MacKinney, E. Woska, I. Spasojevic, I. Batinic-Haberle, R. Zennadi, Disrupting the vicious cycle created by NOX activation in sickle erythrocytes exposed to hypoxia/reoxygenation prevents adhesion and vasoocclusion, *Redox Biol.* 25 (2019) 101097, doi:10.1016/j.redox.2019.101097.
- [55] M. Thamilarasan, R. Estupinan, I. Batinic-Haberle, R. Zennadi, Mn porphyrins as a novel treatment targeting sickle cell NOXs to reverse and prevent acute vasoocclusion in vivo, *Blood Advances* 4 (2020) 2372–2386, doi:10.1182/bloodadvances.2020001642.